Available online at www.sciencedirect.com
SCIENCE DIRECT®
Journal of Pharmaceutical and Biomedical Analysis
31 (2003) 1129–1143
JOURNAL OF PHARMACEUTICAL AND BIOMEDICAL ANALYSIS
www.elsevier.com/locate/jpba

Dissolution of USP prednisone calibrator tablets Effects of stirring conditions and particle size distribution

M. Röst [1], P.-O. Quist *

AstraZeneca Tablet Production Sweden, Quality Assurance and Control, Process Analytical Chemistry, SE-151 85 Södertälje, Sweden

Received 30 September 2002; received in revised form 11 December 2002; accepted 11 December 2002

Abstract

We investigate the effect of stirring conditions on the dissolution of United States Pharmacopoeial Convention (USP) prednisone calibrator tablets. The experiments are performed in an automated USP-II dissolution test apparatus. For this study we use a special paddle-propeller, which can be changed from an ordinary paddle to either a pulling or pushing propeller by changing the angle of the paddle blades. According to the dissolution curves obtained we find that the fastest dissolution, and hence best stirring at a certain stirring frequency, is obtained when the blades of the paddle-propeller is about +30°. This setting corresponds to a pushing, downward flow in the centre of the vessel. We show that the shape of the dissolution curves is similar to that expected from a mix of two different fractions of particles, provided that the stirring is sufficiently intense: one fraction, approximately 60 wt.%, with small particles, and one fraction with large particles. The weight of a large particle is about 100–250 times that of a small. We derive a mathematical expression, based on the cube root law, for the dissolution curves. The expression is fitted to the experimental dissolution curves to investigate the variation of key parameters with stirring and temperature.

Keywords: Stirring; Dissolution; Calibrator tablets; Prednisone; Cube root law; Particle size

1. Introduction

Dissolution analyses have emerged to become one of the fundamental quality tests in the pharmaceutical industry [1–3]. In pharmaceutical production each tablet batch is tested for its dissolution properties, with the intention that they should reflect the bioavailability and bioequivalence of the drug [2–4]. For this purpose, the United States Pharmacopoeial Convention (USP) has developed compendia concerning dissolution standards and policies [5].

The dissolution experiments are sensitive to mechanical and physical–chemical factors [4,6–13]. A typical physical–chemical factor is temperature. The size of the dissolving particles is another important factor, since it reflects the exposed contact area between liquid and solid. The dis-

* Corresponding author.
E-mail address: per-ola.quist@astrazeneca.com (P.-O. Quist).
[1] Present address: AstraZeneca Liquid Production Sweden, S-151 85 Södertälje, Sweden.

0731-7085/03/$ - see front matter
doi:10.1016/S0731-7085(02)00732-X

solution rate also depends on drug solubility, which alone varies according to temperature, molecular structure, different stable polymorph forms and particle size. Mechanical factors could be the position of aliquotation, vibrations, paddle or vessel shape. The unstirred region underneath the paddle has also been shown to contribute to the variability in dissolution [14,15]. Stirring is thus an important factor for the hydrodynamics, which controls the drug removal, and hence the dissolution.

To test and standardise the stirring conditions in dissolution apparatuses one can use dissolution calibrator tablets. USP recommends two different dissolution calibrator tablets: disintegrating (prednisone tablets) and non-disintegrating/eroding (salicylic acid tablets) [5]. To increase the method repeatability the prednisone calibrator tablets are recommended for USP-II (paddle) apparatuses [16,17]. Unfortunately, several collaborative studies have shown that different lots of the prednisone calibrator tablets possess different dissolution behaviour [18–22]. This is thus a factor that must be taken into account at the calibration.

In this paper we investigate the effects of varying the stirring conditions in the automated dissolution test apparatus ACDRA [23,24], which is used for in-process control (IPC) of the dissolution properties of numerous intermediates at AstraZeneca Tablet Production Sweden (TPS). For this purpose we use a specially designed paddle-propeller, which can be changed from a paddle to either a pulling or a pushing propeller. By varying the angle of the paddle blades and the stirring frequency, we investigate the effect of different stirring conditions on the dissolution curve of the USP prednisone calibrator tablets.

In addition to the safety aspects of the dissolution test, there is also a theoretical interest in understanding the dissolution process. The fraction dissolved determined from an in vitro dissolution process of a disintegrating tablet has contributions from many sources [2–4]:

- Initial mechanical lag, e.g. the time it takes for the dissolved substance to reach the detector.
- Wetting of the tablet surface.
- Penetration of the solvent into the tablet.
- Disintegration of the tablet into granules and primary particles.
- Deaggregation, e.g. splitting of clustered particles.
- Dislodgement and occlusion of some particles.

A variety of theoretical dissolution models have been developed to take all these events into account, and to predict the dissolution behaviour [2,3]. The first mathematical expression of a dissolution process was the Noyes–Whitney equation, which describes the dissolution process according to a diffusion-controlled dissolution process [25]. Thirty years later the cube root law was formulated, and it accounted for the decreasing area of the particles during the dissolution process [26,27]. In the present paper we show that, even with intense stirring, the cube root law cannot account for the dissolution profile of the prednisone calibrator tablets. This was not what we initially expected. However, if one assumes that there are (at least) two types or particles in the tablets—for instance small (rapidly dissolving) and large (slowly dissolving)—then it is possible to account for the shape of the dissolution curve. We derive an expression that can be fit to the dissolution curve, and investigate if the parameters in the expression vary as expected with stirring and temperature.

2. Experimental

Unless otherwise stated each dissolution test was performed on two calibrator tablets at 32.0 °C in a 0.050 M phosphate buffer with pH 6.8, using a specially designed paddle-propeller to vary the stirring conditions. Our experimental conditions thus deviate from the recommended procedure with water as a medium, at 37 °C, using an ordinary paddle at 50 rpm. However, from a preliminary study we found that with the selected conditions, the dissolution where more sensitive to the stirring conditions and the properties of the calibrator tablets—which are of interest in this paper.

2.1. Materials

The dissolution experiments were conducted in a 0.050 M aqueous phosphate buffer with pH 6.8. The phosphate buffer was automatically prepared by the ACDRA (cf. below) by mixing 70 wt.% 0.086 M Na_2HPO_4 phosphate solution and 30 wt.% hydrochloric acid solution, according to standardised procedures at AstraZeneca TPS.

The experiments were performed on USP prednisone calibrator tablets (10 mg, disintegrating type), lot N [5] (Promochem AB, Sweden). The calibrator tablets, which are hygroscopic, where stored dry (and dark), because under excess humidity the tablets hardens and the dissolution becomes slower [28]. The repeatability of the dissolution of different lots of prednisone tablets differs. The relative within-a-lot variation of prednisone calibrator tablets has been shown to be between 0.4 and 10.0% [16]. Since no data on the repeatability of lot N was found in literature, we estimated it by repeated experiments.

2.2. Dissolution test

The experiments were performed with the ACDRA dissolution test apparatus [23,24], manufactured by GötaLab, Sweden. The ACDRA apparatus is an automated version of the USP-II dissolution apparatus, with ER/ES-compliant software developed by AstraZeneca TPS. It is used for IPC dissolution tests of various intermediates at AstraZeneca TPS. The concentration of prednisone, released from the calibrator tablets, was measured by UV absorbance at 242 nm, using a Varian Cary 50 UV-Vis spectrophotometer equipped with a flow cell (light path = 10.0 mm) [29]. The flux to the flow cell was continuous and such that it took some 5–6 s to replace about 80% of the content in the cell with new solution from the dissolution vessel. The probe used for aliquotation had a diameter of approximately 2 mm and a length of approximately 20 mm. It was located halfway between liquid surface and the vessel bottom, and about halfway between the vessel wall and the paddle shaft. With this size and location, the probes effect on the dissolution process should be negligible [30–32], which we also have verified (unpublished data). The absorbance was measured once every 30 s during 60 min. The contribution to the absorbance from small particles (turbidity) was removed by an extrapolated linear baseline correction in the spectrum as described elsewhere [24]. The reduced (background-corrected) absorbance was used to calculate the amount of dissolved prednisone using the Beer–Lambert law ($A_{red} = c \times m_{prednisone}$) [33], with the constant determined from a calibration. The dissolution medium was not deaerated [34,35]. To our experience few (or no) bubbles occurred on the particle surfaces, hence deaeration was not necessary.

The fraction dissolved (F) was given in percent of the nominal content of the tablets (2×10 mg). Since the true content varies slightly, the fraction dissolved at the end of the dissolution tests (with intense stirring) was in the range 98–102%, and not exactly 100%.

Each dissolution experiment was performed according to the following procedure, all of which occur automatically according to macros: (a) Wash the vessel and the flow cell (with water purified by reversed osmosis). (b) Fill the vessel and flow cell with dissolution medium. (c) Heat this solution to the proper temperature (usually 32.0 °C) under stirring. (d) Manual addition of two USP calibrator tablets and start of the analysis. (e) Measure the absorbance at 242 nm, and at every 10th nm in the range 350–550 nm. Perform the background correction and calculate the fraction dissolved. Repeat this every 30 s for 1 h. (f) Empty the vessel and wash with water twice. (g) Heat the second portion of water to 57 °C under constant stirring, and empty. (h) An analytical record is generated. Results stored in database. (i) The system is ready for the next analysis.

2.3. Paddle-propeller construction

To investigate the effect of going from paddle stirring to propeller stirring we used a specially designed paddle-propeller in this study—see Fig. 1. The paddle-propeller consisted of two paddle blades, which independently could be twisted and fixed at various angles. It was thus possible to continuously adjust the paddle-propeller from

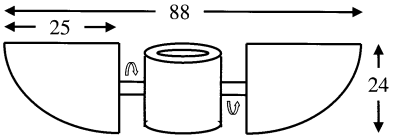

Fig. 1. Cartoon of the paddle-propeller. The paddle-propeller consists of two paddle blades, which independently can be twisted and fixed at various angles. Dimensions are in mm.

sucking flow (blade angle <0, upward flow in the centre of the vessel), to paddle flow (blade angle $=0$), to pushing flow (blade angle >0, downward flow in the centre of the vessel). The blade angles were measured with a goniometer and could be set to within $\pm 3^{\circ}$. The paddle-propeller was adjusted vertically so that the lower edge of the blades was approximately 17 mm above the bottom of the vessel. The size (length) of the blades was adjusted, in an attempt to balance the upward and downward flow of solution, in the following way: when stirring, the sweep-volume (the volume swept by the blades in the paddle position) was approximately equal to the free volume between the sweep-volume and the inside of the vessel. Finally, we like to emphasise that the paddle-propeller should not be compared with a marine propeller, which possesses skewed blades.

2.4. Curve fitting

2.4.1. The dissolution rate

As a simple measure of the rate, of dissolution under different experimental conditions, the software calculated (by a linear least-squares fit) the slope of the dissolution curve in the range $F=20$–50% dissolved. The slope of the best-fit we define as the (dissolution) rate. An example of such a fit is given in Fig. 2. Notice that the dissolution curve is fairly linear in this region.

2.4.2. Non-linear least squares fitting

The rates determined from the initial slope of the dissolution curves are only observed constants, which are difficult to interpret in detail. In order to understand why the dissolution curve varies with stirring and temperature, it was necessary to fit an extended version of the cube root law [26] to the whole dissolution curve. This was performed with

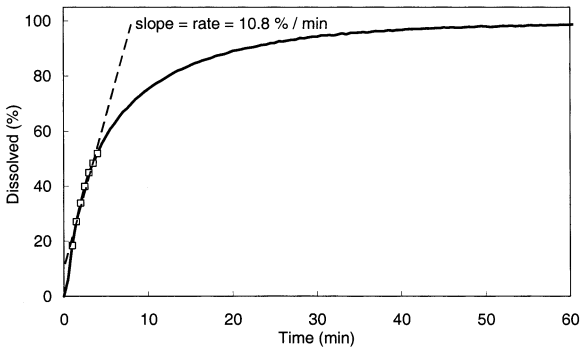

Fig. 2. Best least squares fit of a linear polynomial (hatched line) to the fraction dissolved in the range $F=20$–50% (open diamonds) of the experimental dissolution profile (solid line) of prednisone calibrator tablets. The stirring frequency was 65 rpm and the blade angle 30° (pushing, downward flow in the centre of the vessel).

a non-linear least-squares fit routine written in MATLAB (The MathWorks Inc., USA). The routine is based on the Levenberg–Marquardt minimisation method and is able to fit a defined function, with non-linear parameter dependence, to a specified dataset.

3. Experiments and results

3.1. Experimental repeatability

To investigate the method and tablet repeatability we analysed one, two and four prednisone calibrator tablets in separate dissolution experiments. Six replicates were conducted for each number of tablets. The dissolution tests were performed in 0.050 M aqueous phosphate buffer with pH 6.8 at 37.0 °C with 55 rpm paddle stirring. The fraction dissolved was measured after 5, 10, 20, 30, 40, 50, and 60 min. We found that the standard deviation (S.D.) of the fraction dissolved was essentially the same during the whole dissolution process. For one tablet the S.D. was $\sigma_F=6.1$%-units, for two tablets it was $\sigma_F=4.4$%-units, and for four tablets it was $\sigma_F=2.2$%-units.

If the variation in the dissolution curve is due only to varying properties of the tablets the repeatability should be proportional to $1/\sqrt{n}$, where n is the number of tablets analysed. The

repeatability of four tablets is thus better than expected from the one-tablet and two-tablet repeatability. This indicates that additional factors improve the repeatability when four tablets are analysed. By visual inspection we noticed that with four tablets the shape of the pile of powder under the paddle was more repeatable. With four tablets, the powder pile thus exposes a more constant area, which probably explains the additional improvement in repeatability [9,14]. Notice that in the rest of this study we analysed two tablets in each experiment—although the stirring in many cases was so intense that all material swirled around in the vessel.

There was no significant difference between the average dissolution curves of one, two, and four tablets. According to the Noyes–Whitney equation [25], cf. Eq. (1) below, this indicates that we are working under sink conditions (cf. below).

3.2. Stirring with the paddle-propeller

The study was conducted with two prednisone calibrator tablets in each experiment. The stirring frequencies where 50, 65, 80, 95, and 110 rpm, with the blade angles −75, −60, −45, −30, −15, 0, 15, 30, 45, 60 and 75°. As a measure of the effect of stirring on the dissolution, we used the slope of the dissolution curve in the range $F = 20$–50% dissolved, that is the dissolution rate—see Fig. 2.

The results are given as numbers in Table 1 and as a contour plot in Fig. 3. It is quite clear from Fig. 3 that the fastest dissolution, at a certain stirring rate, is obtained when the blade angle is in the range 15–45° with a pushing (downward) flow

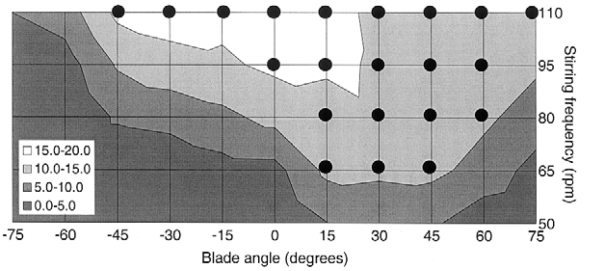

Fig. 3. Contour plot of the observed rate vs. the stirring frequency (y-axis) and the blade angle (x-axis). The black dots indicate the area where the stirring was sufficient for Eqs. (8a), (8b), (8c), (9a), (9b), (9c) and (9d) to describe the experimental dissolution curves.

in the centre of the vessel. This indicates that in this range of blade angles we have the best agitation at a certain stirring frequency—which, without any hydrodynamic calculations, is what one may expect. In a previous study of similar type [36], the authors found that the ordinary paddle resulted in the shortest mixing time of the liquid in the vessel. Shorter mixing times indicate better stirring in the vessel, and hence faster dissolution—in contradiction with our result. However, in that study the authors used an ordinary paddle and some marine propellers. The latter have different hydrodynamics than our paddle-propeller (less turbulence for instance), so the results are not completely comparable.

4. Interpretation of the dissolution curves

In this section we make an attempt to understand the dissolution mechanisms that are respon-

Table 1
The dissolution rate at different stirring frequencies and blade angles

Stirring (rpm)	Blade angle (°)										
	−75	−60	−45	−30	−15	0	15	30	45	60	75
50	0.1	0.2	0.2	0.3	0.3	0.4	4.9	7.0	5.8	1.6	0.3
65	0.1	0.2	0.4	1.9	3.2	3.3	11.2	10.8	11.2	8.2	3.1
80	0.2	0.4	5.8	6.5	8.7	11.6	13.5	14.7	13.1	10.9	7.9
95	0.2	2.8	10.5	13.2	14.2	16.0	15.5	14.7	14.1	13.1	10.7
110	5.1	7.4	16.2	17.2	16.3	17.4	15.7	14.5	13.7	14.6	13.5

The rate is given in % min^{-1}.

sible for the variation seen in Fig. 3. Therefore, we shall review some of the basic papers on dissolution.

4.1. The Noyes–Whitney equation

The fundamental law concerning the rate at which solids dissolve 'in their own solutions' is the Noyes–Whitney equation [25] published in 1897. The equation states that the rate of concentration change at any instant (dC/dt) is proportional to the difference between the concentration (C) and the solubility (C_S), that is

$$\frac{dC}{dt} = k(C_S - C). \quad (1)$$

The conditions set to derive this equation cause some restrictions for the expression. For practical work with pharmaceutical tablets, an important restriction is the assumption of a constant area (a) of the solid in contact with the solution. Another is the assumption about sufficiently intense stirring. In the derivation it was also assumed that the concentration at the particle surface is equal to the solubility (C_S).

If the stirring is sufficiently intense, the rate-limiting process of the dissolution is, in many cases, the diffusive transport of the solute from a thin film of saturated solution, at the solid, into the bulk [4]. In this case the rate constant (k) is given by [37]

$$k \propto \frac{Da}{hV}, \quad (2)$$

where D is the diffusion coefficient (normal to the solid surface) of the solute in the saturated solvent, h is the thickness of the diffusion layer outside the solid surface (the 'stagnant layer'), and V is the volume of the solvent. The stagnant layer is a result of a simple two-state model where two types of molecular flux (from the particle surface, along the surface normal, into the bulk) are considered—diffusive (near the surface) and convective (in the bulk liquid). The thickness of the stagnant layer (h) can, therefore, be thought of as the (hypothetical) distance were the diffusive flux, of molecules dissolved at the surface, becomes smaller than the convective flux [37]. This implies, for instance, that an increased stirring results in a reduction of the thickness of the stagnant layer. Since the stagnant layer is a result of a simplification, its exact thickness (h) is of little interest. According to some experimental studies the thickness of the stagnant layer seems to be in the range $h \approx 30$–60 μm, or so [38–42], under ordinary stirring conditions. If the stirring is intense, the thickness of the stagnant layer is less.

4.2. The cube root law

If one prefers to analyse the full dissolution curve there are numerous equations to consider [2,3]. Some of these, for instance the cube root law, have been derived from simple and reasonable physical considerations. For the disintegrating prednisone calibrator tablets, the cube root law should be a suitable choice. This is because the tablets rapidly disintegrate (within seconds) into primary particles of the substance and excipients. The cube root law, which was derived in 1931 by Hixson and Crowell [26,27], describes the dissolution of a solid particle (or a number of identical particles) in a solvent. By assuming that no, or little, happened to the shape of particle(s) during the dissolution, it was possible to account for the decreasing area of dissolving particles. Under sink conditions ($C_S \gg C$), the cube root law reads, in the original notation, [26]

$$k_4(t - t_{lag}) = w_0^{1/3} - w^{1/3}. \quad (3)$$

In Eq. (3) w_0 is the initial weight of the particle, w is the weight of the particle at time t, and k_4 is a rate constant. In Eq. (3) we have added t_{lag}, which is a lag-time that accounts for initial processes of the dissolution (for instance tablet disintegration). As shown in Section 3, we performed our experiments under sink conditions ($C_S \gg C$), and under a wide range of stirring conditions, some of which we expect to be sufficiently intense to make diffusive transport rate-limiting. If diffusive transport is the rate-limiting process of the dissolution, the rate constant k_4 is proportional to

$$k_4 \propto \frac{q\rho^{2/3} C_S D}{h}, \tag{4}$$

where ρ is the density of the particle, and q its shape factor [26], defined by

$$q = \frac{a}{v^{2/3}}, \tag{5}$$

where a and v is the initial area and volume, respectively, of the particle.

The shape factor in Eq. (5) is easy to calculate for simple geometries like cubes and spheres. On the other hand, if there are pores in the surface of a particle, they increase the area, which according to Eq. (5) should yield a large shape factor. However, if the size of a pore is smaller than the thickness of the stagnant layer, there is no convective flux into the pore, which thus contains a saturated solution. The concentration gradient outside this pore will, therefore, look the same as if there was no pore. In the spirit of the cube root law, this means that small pores (< thickness of stagnant layer) should be omitted when the area of the particle is estimated. The area of the particle and the shape factor can thus be estimated quite correctly by using simple geometries. For example, a spherical particle, which has the smallest shape factor, $q_{\text{sphere}} \approx 4.8$, whereas a cubical particle has $q_{\text{cube}} = 6$. For more extended geometries the surface to volume ratio increases, yielding larger shape factors. For instance, a rod-like particle with a length that is ten times the diameter of its circular cross section has $q_{\text{rod}} \approx 8.3$, and a flake-like particle with a diameter that is ten times its thickness has $q_{\text{flake}} \approx 10$. From these examples we expect the shape factor to be within the range $q \approx 5$–10, unless the substance particles are very extended.

In the derivation of Eqs. (3)–(5) the following assumptions were made [26]:

a) The dissolution process is rate-limited by a diffusion process, which occur normal to the surface of the particle(s).
b) The particle shape is predominantly spheroid-like and constant during the dissolution. In practise this means that the particle has convex surfaces, and that it is not extremely extended (otherwise its shape will change too much during the dissolution).
c) The stirring is sufficiently intense to immediately distribute the solutes dissolved from the stagnant layer into the bulk, and that the stirring affects all surfaces of the particles equally.
d) All particles have the same shape and initial weight—if more than one particle is analysed.
e) Sink conditions, that is $C_S \gg C$.

When these assumptions are fulfilled in practise, the cube root law usually describes the dissolution process up to about 85% dissolved or more [27]. Deviation from linearity beyond this limit commonly originates from differently sized particles [26,27]. This is because small particles expose by far larger areas to the solvent compared with larger particles. Therefore, small particles dissolve at an earlier stage of the dissolution process, and large particles dominate towards the end of the dissolution process.

The original form of the cube root law (Eq. (3)) was derived to yield a linear variation with time. Today it is more common to present analytical results as the fraction dissolved (F) versus time. Since the dissolution process ends when 100% of the content have been released, it is simple to rewrite Eq. (3) into this form if one recognises that

$$F = 100\frac{w_{\text{dissolved}}}{w_0} = 100\frac{w_0 - w}{w_0}, \tag{6a}$$

and hence

$$w = w_0\left(1 - \frac{F}{100}\right). \tag{6b}$$

By replacing w in Eq. (3) by the expression in Eq. (6b) we obtain

$$k_4(t - t_{\text{lag}}) = w_0^{1/3} - w_0^{1/3}\left(1 - \frac{F}{100}\right)^{1/3}, \tag{6c}$$

which we can solve for F, yielding

$$F = 100\left\{1 - \left[1 - \frac{k_4(t - t_{\text{lag}})}{w_0^{1/3}}\right]^3\right\}, \tag{7}$$

which gives the fraction dissolved (F in %) for a number of identical solid particles, each having the

initial weight w_0. Eq. (7) is valid in the range $0 \leq F \leq 100$. If the calculated value of $F < 0$, then F should be set to 0, and if the calculated value of $F > 100$, it should be set to 100. In Appendix A we give an example of a MATLAB function that fulfils these requirements.

4.3. Fitting the cube root law to dissolution curves

Eq. (7) can be used for non-linear least-squares curve fitting to experimental dissolution profiles. In Fig. 4, we show the best-fit of Eq. (7) to the dissolution profile of two USP prednisone calibrator tablets. The stirring frequency was 110 rpm and the blade angle 0° in order to have sufficiently intense stirring (which in practise means that all particles swirl around in the vessel).

As we can see in Fig. 4, the best least-squares fit of Eq. (7) to the dissolution curve is not very good. It seems as if the experimentally observed dissolution is faster than predicted by the cube root law initially, and slower at the end. This can be verified if we fit Eq. (7) separately to the initial (0–2 min) and final (10–40 min) parts of the dissolution curve—see Fig. 4. The values of the parameters, in Eq. (7), obtained from the three fits in Fig. 4 are given in Table 2. Notice that the rate constants

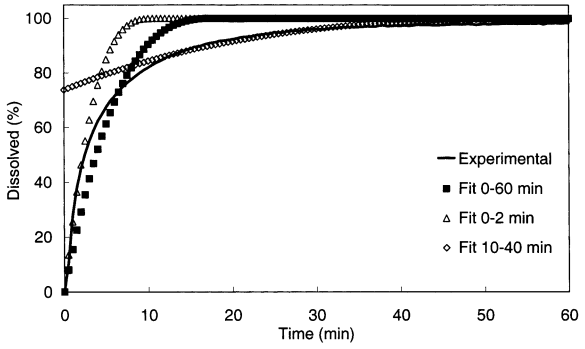

Fig. 4. Best non-linear least-squares fits of Eq. (7) to various parts of the experimental dissolution profile (solid line) of prednisone calibrator tablets. The temperature was 32.0 °C, the stirring 110 rpm, and the blade angle 0° (paddle). Solid squares: best-fit to the complete dissolution profile. Open triangles: best-fit to the initial part (0–2 min) the dissolution profile. Open diamonds: best-fit to the final part (10–40 min) the dissolution profile.

derived at the end and beginning of the dissolution profile differs by about a magnitude.

It might be somewhat puzzling that the cube root law can not describe the dissolution curve better. There could be several explanations:

i) The shape factor (q) may vary—see Eq. (5). However, the rate constant appears to vary by a factor of 10, or so, which is much more than we expect from changes in the shape of the particles (cf. the discussion above).
ii) Another reason could be insufficient stirring. This is, however, not likely—the stirring was intense, and all particles swirled around everywhere in the vessel.
iii) Another cause may be that the dissolution is not rate limited by the diffusion process. However, as stated already by Hixson and Crowell [26], this is actually not necessary—the mathematical expression will still look like Eq. (7), though the interpretation of the rate constant in Eq. (4) (k_4) would be different.

Hixson and Crowell suggested that the most likely explanation to deviations from the cube root law is the presence of two types or sizes of particles. For us this means (at least) two types or sizes of particles in the prednisone calibrator tablets—one fraction of particles with fast release, and another fraction with a slower release. The fraction with the fast release must be particles that are small (small w_0) and/or have a large area per volume (large q).

4.4. Cube root law for two fractions

Let us, therefore, assume that there are two types of particles in the USP prednisone calibrator tablets, namely A- and B-type particles. For each of them Eq. (7) is valid as long as we have sink conditions (because then there is no coupling to the total concentration). Therefore, we have

$$F = A[Q_A F_A + (1 - Q_A) F_B], \tag{8a}$$

$$F_A = \{1 - [1 - k_A(t - t_{lag})]^3\}, \tag{8b}$$

$$F_B = \{1 - [1 - k_B(t - t_{lag})]^3\}. \tag{8c}$$

Here, A is the final amplitude of the dissolution curve, which we expect to be 100% of the nominal

Table 2
Values of the parameters, in Eq. (7), obtained at the three fits in Fig. 4

Part of dissolution curve fitted (min)	t_{lag} (min)	$k_4/w_0^{1/3}$ (min^{-1})	dY (%-units)[a]
0–60	0.0	0.054	6.2
0–2	0.0	0.093	2.0
10–40	−35.7[b]	0.010	0.8

[a] Computed S.D. for the difference between the best-fit and the experimental dissolution curve.
[b] It was necessary to allow the lag-time to be non-zero in order to obtain a reasonable fit.

content. However, minor variations in the actual content of the tablets may yield a slightly different value. Q_A and $Q_B = (1 - Q_A)$ are the weight fractions of the A- and B-type of particles, respectively. F_A and F_B are limited to the range $0 \le F_A$, $F_B \le 1$, for the same reason as F, in Eq. (7) is limited to the range 0–100. In Eqs. (8a), (8b) and (8c) k_A and k_B are the rate constants, which are given by

$$k_A = \varsigma \frac{q_A}{w_{0A}^{1/3}}, \tag{9a}$$

$$k_B = \varsigma \frac{q_B}{w_{0B}^{1/3}} = \hat{c} k_A, \tag{9b}$$

with the constants given by

$$\varsigma \propto \frac{\rho^{2/3} C_S D}{h}, \tag{9c}$$

and

$$\hat{c} = \frac{w_{0A}^{1/3}}{q_A} \frac{q_B}{w_{0B}^{1/3}}. \tag{9d}$$

In Eq. (9d) $\hat{c}$ is a weight–shape ratio of the A-particles with respect to the B-particles. All other parameters have the same meaning as before, though an A or a B now indexes them. Notice that in order to derive Eqs. (9a), (9b), (9c) and (9d) we have assumed that the only things that differ between the two types of particles are their size and shape. Therefore, the rate-limiting diffusion process is the same independently of their size and shape.

The number of unknown parameters in Eqs. (8a), (8b), (8c), (9a), (9b), (9c) and (9d) is quite small: A, Q_A, t_{lag}, k_A, and $\hat{c}$. Of these, it is obvious from the experimental dissolution curves that the lag-time (t_{lag}) is essentially zero. Furthermore, the amplitude ($A \approx 100$) is determined from the value of F as it levels off at the end of the dissolution process. This means that there are only three truly unknown parameters to fit. Of these, Q_A is a property of the tablets, and we expect it to have the same value for all tablets (at least if they are from the same lot). Once Q_A has been determined, the only parameters affecting the dissolution process are the rate constant (k_A) and the weight–shape ratio of the A- to B-type particles ($\hat{c}$). The MATLAB function corresponding to Eqs. (8a), (8b), (8c), (9a), (9b), (9c) and (9d) is given in Appendix B.

In Fig. 5 we show the best-fit of Eqs. (8a), (8b), (8c), (9a), (9b), (9c) and (9d) to the same dissolution curve as in Fig. 4—as we can see the fit is much better than the ones in Fig. 4, though it is not perfect. We believe that the small difference, between the experimental dissolution curve and

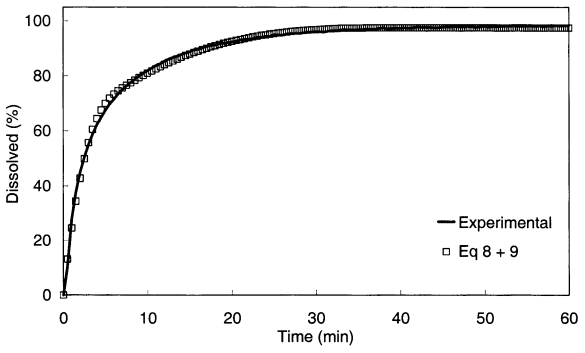

Fig. 5. Best non-linear least-squares fits of Eqs. (8a), (8b), (8c), (9a), (9b), (9c) and (9d) to the experimental dissolution profile (solid line) of prednisone calibrator tablets. The computed S.D. for the difference between the best-fit and the experimental curve (dY) is about 1.5%-units. Open squares: best-fit to the full dissolution profile.

the best-fit, is due to minor variations in the size and shape within the two sorts (A- and B-type) of particles, respectively. The numbers derived should thus be regarded as average properties of the two fractions. From the best-fit we obtain $Q_A = 0.60$, $k_A = 0.14$ (min^{-1}), and $\hat{c} = 0.17$. Since the dissolution begins immediately the lag-time was set to 0, and because the curve level off at $F = 97.5\%$ released, the amplitude was set to 97.5 rather than 100. If we assume that the shape of the A- and B-type particles is approximately the same ($q_A \approx q_B$), then $\hat{c} = 0.17$ means that $w_{0B}/w_{0A} \approx 200$ (see Eq. (9d)). It thus seems as if the prednisone calibrator tablets contain two sorts of prednisone particles: approximately 60 wt.% of them are small and 40 wt.% of them are about 200 times heavier than the small ones. The small particles may be splinters and flakes torn off from the large particles at compaction of the tablets, or occur already in the substance at granulation.

4.5. Estimating the fraction small particles, Q_A

As mentioned we expect the fraction of small particles (Q_A) to be constant, since it is a property of the prednisone calibrator tablets. To determine Q_A we fitted Eqs. (8a), (8b), (8c), (9a), (9b), (9c) and (9d) to the dissolution profiles obtained at high stirring frequency (>80 rpm) and small positive blade angles. The results from these best-fits are given in Table 3. Since all dissolution curves did not show any presence of a lag-time, and they levelled of at $F \approx 100\%$, we performed the fits with $t_{lag} = 0$ and $A = 100$. As expected there was almost no variation in Q_A—the relative standard deviation (R.S.D.) was about 2%. The small S.D. verifies that Q_A is constant and a property of this lot of tablets. Hence we can conclude that the weight fraction small particles in the USP prednisone calibrator tablets is $Q_A = 0.60$. Hereafter we lock Q_A to this value.

In Table 3 we notice that the rate constant k_A and the weight–shape ratio $\hat{c}$ vary by about 10 and 5%, respectively. It thus seems as if they depend on the stirring in some sense. For the rate constant this is likely an effect of the stirring on the thickness of the stagnant layer (h) [37]—see Eqs. (9a) and (9c). Another conclusion we can draw is that Eqs. (8a), (8b), (8c), (9a), (9b), (9c) and (9d) are able to describe the dissolution curve quite well—the computed S.D. for the difference between the best-fit and the experimental curve (dY) is about 1%-unit, which should be compared with the 6.2%-units for original form of the cube root law in Eq. (7) (see Table 2).

4.6. Effects on the dissolution by stirring

To judge if Eqs. (8a), (8b), (8c), (9a), (9b), (9c) and (9d) together constitute a good model for the dissolution of prednisone from the calibrator tablets, one can vary one or several parameters and check if the response of the model appears to

Table 3
Results from best-fit of Eqs. (8a), (8b), (8c), (9a), (9b), (9c) and (9d) to experimental dissolution curves

Stirring (rpm)	Blade angle (°)	k_A (min^{-1})	Q_A	$\hat{c}$	dY (%-units)[a]
110	15	0.148	0.612	0.147	1.6
110	30	0.138	0.596	0.163	1.2
110	45	0.140	0.588	0.159	1.4
110	60	0.125	0.595	0.161	1.4
95	15	0.133	0.600	0.168	1.2
95	30	0.130	0.587	0.160	1.4
95	45	0.115	0.628	0.151	1.8
80	15	0.109	0.607	0.168	1.4
Average		0.130	0.602	0.160	
S.D.		0.013	0.014	0.007	

$t_{lag} = 0$; $A = 100$
[a] Computed S.D. for the difference between the best-fit and the experimental dissolution curve.

be what one expected. In this section we check how k_A and $\hat{c}$ vary with the stirring.

In Fig. 6 we show the dissolution curves obtained, with the blade angle of the paddle-propeller being 15° (pushing, downward flow), at different stirring frequencies. As we can see, the curve obtained at 50 rpm levels off at $F \approx 75\%$ dissolved, which indicates that some substance particles are hidden in the small pile that appeared at the bottom of the vessel in this experiment.

Since the dissolution begins immediately, we set $t_{lag} = 0$. Furthermore, we expect about 100% dissolved at the end of the experiments—otherwise the stirring has been too slow. Therefore, only the dissolution curves where $F > 98\%$ at the end are considered. Finally, Q_A is set to 0.60, as determined in the previous section. In Eqs. (8a), (8b), (8c), (9a), (9b), (9c) and (9d), there are then only two parameters to fit: k_A and $\hat{c}$. The stirring conditions where it was possible to fit Eqs. (8a), (8b), (8c), (9a), (9b), (9c) and (9d) to the dissolution curves are shown as black dots in Fig. 3. The covariance with the observed rate constant in this figure is striking. The area covered by the black dots can thus be identified as the region where the stirring is sufficient for Eqs. (8a), (8b), (8c), (9a), (9b), (9c) and (9d) to be valid. That is, the region where diffusion through the stagnant layer is the rate-limiting step of the dissolution. The remaining area is the region where the stirring is not sufficiently intense to immediately distribute the solutes diffusing from the stagnant layer into the bulk.

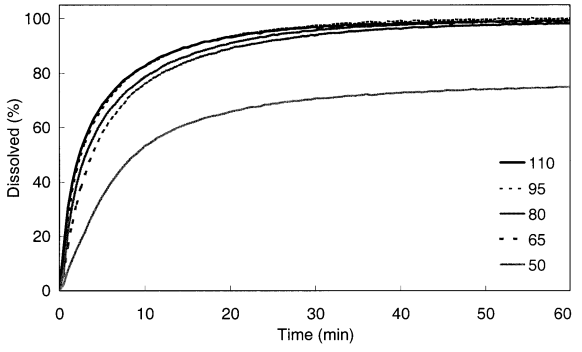

Fig. 6. Dissolution curves of prednisone calibrator tablets obtained with 15° blade angle (pushing, downward flow) at stirring frequencies 50, 65, 80, 95, and 110 rpm. The dissolution rate increases with the stirring frequency.

In Tables 4 and 5 we show the values we obtained for k_A and $\hat{c}$, respectively. The uncertainty, in both parameters, is estimated to approximately ± 0.01. The computed S.D. for the difference between the best-fit and the experimental curve (dY) was 1.4%-units or less, which indicates that the equations really can take the same shape as the dissolution curves.

As we can see in Table 4, k_A increases as the stirring becomes more intense. We interpret this as a decreasing thickness of the stagnant layer (h) as the stirring increases [4,37]—see Eq. (9c).

The weight–shape ratio $\hat{c}$ in Table 5 displays an opposite trend with the stirring: $\hat{c}$ decreases slightly as the stirring increases. If we assume that q_B/q_A is independent of stirring the decrease in $\hat{c}$ is due solely to a change in the weight ratio (w_{0B}/w_{0A}). The trend then corresponds to an increase in w_{0B}/w_{0A} from 100 to 250 as the stirring increases. If, on the other hand, we assume that w_{0B}/w_{0A} is independent of stirring the decrease in $\hat{c}$ is due solely to a decrease in the shape ratio (q_B/q_A). The trend then corresponds to a decrease in q_B/q_A by about 25% as the stirring increases. In the dissolution vessel some of the large particles will be hit (or sheared) by the paddle blades. We also expect the number of hits and the transferred energy in each hit to increase with the stirring frequency. Each hit may tear of small pieces from the large particles. This reduces their weight and shape factor (and increases the fraction small particles (Q_A) slightly). If the weight of the large particles decreases then w_{0B}/w_{0A} decreases with increased stirring, which is opposite to what we observe. If the shape factor of the large particles decreases, then q_B/q_A decreases—as observed. Since $\hat{c}$ is equal to $(q_B/q_A)(w_{0B}/w_{0A})^{-1/3}$, we expect q_B/q_A to dominate the variation in $\hat{c}$. The decrease in $\hat{c}$ with increased stirring can thus be understood as caused by slight erosion of the large particles.

The variation seen in k_A and $\hat{c}$ is thus of the type one might expect—which indicates that the assumptions underlying Eqs. (8a), (8b), (8c), (9a), (9b), (9c) and (9d) are appropriate for the dissolution of the prednisone calibrator tablets (at intense stirring).

Table 4
k_A (min^{-1}) derived from a non-linear least squares fit of Eqs. (8a), (8b), (8c), (9a), (9b), (9c) and (9d) to the dissolution curves as described in the text

Stirring (rpm)	Blade angle (°)										
	−75	−60	−45	−30	−15	0	15	30	45	60	75
50											
65							0.09	0.09	0.09		
80							0.11	0.11	0.11	0.10	
95						0.12	0.13	0.13	0.12	0.11	
110			0.12	0.12	0.14	0.14	0.15	0.14	0.14	0.12	0.10

Empty cells indicate that it was not possible to fit the equations to the dissolution curve.

4.7. Temperature dependence of k_A

A second test on the assumptions underlying Eqs. (8a), (8b), (8c), (9a), (9b), (9c) and (9d) is the temperature dependence of the rate constants k_A (and k_B). The temperature variation in k_A and k_B occur actually in the common coefficient ς—see Eq. (9c). To investigate the temperature dependence of the dissolution, we repeated the experiments performed with the blade angle at 30° and the stirring at 65, 80, 95, and 110 rpm, but now at 42.0 and 52.0 °C. Eqs. (8a), (8b), (8c), (9a), (9b), (9c) and (9d) were fitted to the dissolution curves as described in the previous section. The fraction small particles was set to $Q_A = 0.60$. At 42.0 and 52.0 °C we obtained the same weight–shape ratio ($\hat{c}$) as we did at 32.0 °C (cf. Table 5)—if the propagated experimental uncertainties were taken into account. The rate constant k_A, on the other hand, increased with temperature as shown in Fig. 7. On average we found that a temperature increase of 20 °C, increased k_A (that is, the coefficient ς) by a factor of 2.0.

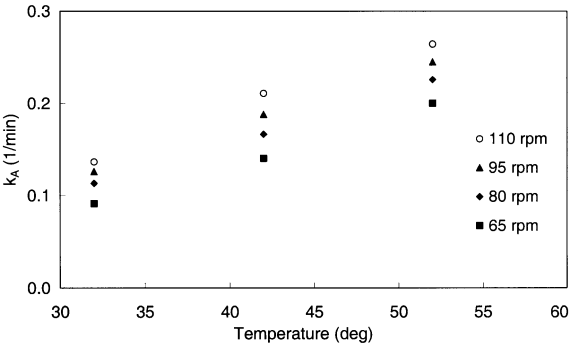

Fig. 7. Temperature variation in the rate constant k_A at 65, 80, 95, and 110 rpm stirring frequency. The blade angle was set to 30° (pushing, downward flow in the centre of the vessel).

In the coefficient ς there are three parameters that are dependent on the temperature (see Eq. (9c)): The solubility (C_S) and the diffusion coeffi-

Table 5
$\hat{c}$ derived from a non-linear least squares fit of Eqs. (8a), (8b), (8c), (9a), (9b), (9c) and (9d) to the dissolution curves as described in the text

Stirring (rpm)	Blade angle (°)										
	−75	−60	−45	−30	−15	0	15	30	45	60	75
50											
65							0.21	0.19	0.20		
80							0.18	0.17	0.17	0.18	
95						0.18	0.17	0.17	0.17	0.18	
110			0.18	0.19	0.18	0.17	0.16	0.17	0.17	0.17	0.18

Empty cells indicate that it was not possible to fit the equations to the dissolution curve.

cient (D), which we expect to increase with temperature, and the thickness of the stagnant layer (h). The temperature dependence of the latter is difficult to estimate. King [37] argued that h should be essentially independent of the viscosity of the solution, as long as the density was constant, which means that it should be essentially independent of temperature. Anyhow, we can write the following general ratio for k_A at 52.0 and 32.0 °C (using Eqs. (9a) and (9c)).

$$\frac{k_A^{52C}}{k_A^{32C}} = \frac{D^{52C}}{D^{32C}} \frac{C_S^{52C}}{C_S^{32C}} \frac{h^{32C}}{h^{52C}} \approx \frac{\eta^{32C}}{\eta^{52C}} \frac{C_S^{52C}}{C_S^{32C}} \frac{h^{32C}}{h^{52C}}. \quad (10)$$

In the latter equality we have approximated the temperature dependence of the diffusion coefficient of prednisone, with that of the viscosity of bulk water (which is the solvent in the stagnant layer), that is $D \propto 1/\eta$ [33]. According to the literature [43] $(\eta^{32C}/\eta^{52C}) \approx 1.4$ for water. Unfortunately, we have not been able to find the temperature dependence of C_S (for prednisone in water) in the literature. However, that of budesonide, which has a similar molecular structure and solubility, can approximate it. Therefore, we set $(C_S^{52C}/C_S^{32C}) \approx 2$ [44]. Since we experimentally have found that $k_A^{52C}/k_A^{32C} = 2$, it is necessary that $(h^{32C}/h^{52C}) \approx 1/1.4 \approx 0.7$ for Eq. (10) to hold. According to King we should expect $(h^{32C}/h^{52C}) \approx 1$ [37]. With the approximations done and the limitations underlying the cube root law we find these small differences satisfactory. The temperature dependence of k_A thus indicates that the assumptions underlying Eqs. (8a), (8b), (8c), (9a), (9b), (9c) and (9d) are appropriate for the dissolution of prednisone from the USP prednisone calibrator tablets.

5. Conclusions

The variation in the dissolution curves, of USP prednisone calibrator tablets, with stirring conditions have shown that the fastest dissolution, and hence best stirring, is obtained when the blades of the paddle-propeller is about +30° (pushing, downward flow in the centre of the vessel). This is in contradiction with earlier results [36], showing that a paddle (blade angle = 0°) gave the best stirring in the vessel.

In addition we have shown that, in the range with sufficient stirring, the dissolution curves from the USP prednisone calibrator tablets can be described by a cube root law including particles with two sizes: approximately 60 wt.% small particles and approximately 40 wt.% large particles. The weight of the latter is about 100–250 times that of the small ones. Probably there is a distribution in the size and shape within each of the fractions of small and large particles, respectively.

It is well known that different lots of prednisone calibrator tablets possess varying dissolution behaviour, which have been addressed in several collaborative studies [18–22]. We suggest that this might be due to varying fractions, or sizes, of the small and large particles. To obtain a more reproducible dissolution behaviour of the prednisone calibrator tablets, the size distribution and/or mechanical properties of the substance and granule particles should be better characterised at manufacturing.

Appendix A: MATLAB function for Eq. (7)

```
function Y = cuberoot(X,P)
% X = time vector
% Y = fraction dissolved vector
A = P(1); % Amplitude. Usually = = 100.
K = P(2); % = k4/w0^1/3
T = P(3); % Lag-time. Usually = = 0.
y = (1-(1-K*(X-T)).^3);
for k = 1:length(X)
   if y(k) < 0 % Test if y < 0
      y(k) = 0;
end
if y(k) > 1 % Test if y > 1

      y(k) = 1;
   end
end
Y = A*y;
```

Appendix B: MATLAB function for Eqs. (8a), (8b), (8c), (9a), (9b), (9c) and (9d)

```
function Y = cuberoot2(X,P)
% X = time vector
% Y = fraction dissolved vector
A = P(1); % Amplitude. Usually = =100.
KA = P(2); % Rate constant for A-type particles
T = P(3); % Lag-time. Usually = =0.
QA = P(4); % Weight fraction A-type particles
C = P(5); % Weight–shape quotient of A- to B-type particles
KB = C*KA;
QB = 1-QA;
yA = (1-(1-KA*(X-T)).^3); % Dissolution of A-type particles
for k = 1:length(X)
   if yA(k) < 0
      yA(k) = 0;
   end
   if yA(k) > 1
      yA(k) = 1;
   end
end
yB = (1-(1-KB*(X-T)).^3); % Dissolution of B-type particles
for k = 1:length(X)
   if yB(k) < 0
      yB(k) = 0;
   end
   if yB(k) > 1
      yB(k) = 1;
   end
end
y = QA*yA+QB*yB;
Y = A*y;
```

References

[1] J.L. Cohen, B.B. Hubert, L.J. Leeson, C.T. Rhodes, J.R. Robinson, T.J. Roseman, E. Shefter, Pharm. Res. 7 (1990) 983–987.

[2] U.V. Banakar, M.C. Makoid, Drug Dissolution and Bioavailability (Seminar handouts), Technomic Publishing AG, Basel, Switzerland, 1994.

[3] J.D. Dressman, H. Lennernäs, Oral Drug Absorption—Prediction and Assessment, Marcel Dekker, New York, 2000.

[4] M.E. Aulton, Pharmaceutics: The Science of Dosage Form Design, Churchill Livingstone, London, 1998.

[5] The United States Pharmacopeia 24, NF 19, United States Pharmacopeial Convention Inc., Rockville, USA, 2000.

[6] D.C. Cox, C.C. Douglas, W.B. Furman, R.D. Kirchhoefer, J.W. Myrick, C.E. Wells, Pharm. Technol. 4 (1978) 41–53.

[7] K.D. Thakker, N.C. Naik, V.A. Gray, S. Sun, Pharm. Forum 2 March–April (1980) 177–185.

[8] D.C. Cox, C.E. Wells, W.B. Furman, T.S. Savage, A.C. King, J. Pharm. Sci. 71 (1982) 395–399.

[9] D.C. Cox, W.B. Furman, J. Pharm. Sci. 71 (1982) 451–452.

[10] D.C. Cox, W.B. Furman, L.K. Thornton, T.W. Moore, E.H. Jefferson, J. Pharm. Sci. 72 (1983) 910–913.

[11] D.C. Cox, W.B. Furman, T.W. Moore, C.E. Wells, Pharm. Technol. 8 (1984) 43–46.

[12] V.A. Gray, B.B. Hubert, Pharm. Forum 20 (1994) 8571–8573.

[13] T.W. Moore, R.F. Shangraw, Y. Habib, Pharm. Forum 22 (1996) 2423–2428.

[14] F.L. Underwood, D.E. Cadwallader, J. Pharm. Sci. 65 (1976) 697–700.

[15] A.H. Beckett, T.T. Quach, G.S. Kurs, Dissol. Technol. 3 (1996) 7–18.

[16] S.A. Qureshi, I.J. McGilveray, Drug Dev. Ind. Pharm. 21 (1995) 905–924.

[17] S.A. Qureshi, Drug Inf. J. 30 (1996) 1055–1061.

[18] D.C. Cox, W.B. Furman, J. Pharm. Sci. 73 (1984) 670–675.

[19] T.W. Moore, J.F. Hamilton, C.M. Kerner, Pharm. Forum 21 (1995) 1387–1396.

[20] A.S. Achanta, V.A. Gray, T.L. Cecil, L.T. Grady, Drug Dev. Ind. Pharm. 21 (1995) 1171–1182.

[21] H. Blume, S.A. Qureshi, S.L. Ali, I.J. McGilveray, Drug Dev. Ind. Pharm. 21 (1995) 925–943.

[22] S.A. Qureshi, I.J. McGilveray, Eur. J. Pharm. Sci. 7 (1999) 249–258.

[23] G. Zackrisson, G. Östling, B. Skagerberg, T. Anfält, J. Pharm. Biomed. Anal. 13 (1995) 377–383.

[24] P.-O. Quist, G. Östling, J. Pharm. Biomed. Anal. 28 (2002) 1081–1089.

[25] A.A. Noyes, W.R. Whitney, J. Am. Chem. Soc. 19 (1897) 930–934.

[26] A.W. Hixon, J.H. Crowell, Ind. Eng. Chem. 23 (1931) 923–931.

[27] A.W. Hixon, J.H. Crowell, Ind. Eng. Chem. 23 (1931) 1002–1009.

[28] C.J. Taborsky-Urdinola, V.A. Gray, L.T. Grady, Am. J. Hosp. Pharm. 38 (1981) 1322–1327.

[29] C. Buhlmann, Spectr. Eur. 12 (2000) 18–23.

[30] C.E. Wells, J. Pharm. Sci. 70 (1981) 232–233.

[31] T.S. Savage, C.E. Wells, J. Pharm. Sci. 71 (1982) 670–673.

[32] I. Nir, B.D. Johnson, J. Johansson, C. Schatz, Pharm. Technol. Eur. 3 (2002) 20–28.
[33] P.W. Atkins, Physical Chemistry, Oxford University Press, Oxford, 1998.
[34] D.C. Cox, W.B. Furman, D.P. Page, J. Pharm. Sci. 72 (1983) 1061–1064.
[35] S.A. Qureshi, I.J. McGilveray, Pharm. Forum 20 (1994) 8565–8566.
[36] M. Lagas, C.F. Lerk, Pharm. Weekbl. 113 (1978) 1277–1282.
[37] C.V. King, J. Am. Chem. Soc. 57 (1935) 828–831.
[38] W.I. Higuchi, E.L. Parrott, D.E. Wurster, T. Higuchi, J. Am. Pharm. Assoc. 47 (1958) 376–383.
[39] W.E. Hamlin, E. Nelson, B.E. Ballard, J.G. Wagner, J. Pharm. Sci. 51 (1962) 432–435.
[40] G. Levy, J. Pharm. Sci. 52 (1962) 1039–1046.
[41] W.E. Hamlin, J.I. Northam, J.G. Wagner, J. Pharm. Sci. 54 (1965) 1651–1653.
[42] W.I. Higuchi, P.D. Bernardo, S.C. Mehta, J. Pharm. Sci. 56 (1967) 200–207.
[43] R.C. Weast, Handbook of Chemistry and Physics, 57th ed, CRC Press, Boca Raton, USA, 1976.
[44] U. Espmarker, AstraZeneca R&D Lund, Sweden, Personal communication.